ARTICLE

Ethylene Adsorption on Ag(111), Rh(111) and Ir(111) by (meta)-GGA based Density Functional Theory Calculations

Pei-pei Chen[a,d], Bing-yan Zhang[a,d], Xiang-kui Gu[b], Wei-xue Li[c*]

a. State Key Laboratory of Catalysis, Dalian Institute of Chemical Physics, Chinese Academy of Sciences, Dalian 116023, China
b. Department of Chemical Engineering and Materials Science, Wayne State University, Detroit, MI 48202, USA
c. Department of Chemical Physics, College of Chemistry and Materials Science, University of Science and Technology of China, Hefei National Laboratory for Physical Sciences at the Microscale, Hefei 230026, China
d. University of Chinese Academy of Sciences, Beijing 100049, China

Accurate description of the adsorption process of reactants on metal surfaces from theory is crucial for mechanistic understanding of activity and selectivity of metal catalysts, but it remains challengeable for the nowadays first-principles theory due to the lack of proper exchange-correlation functional describing the distinct interactions involved. We studied here the potential energy surfaces of ethylene adsorption on Ag(111), Rh(111) and Ir(111) using density functional theory calculations and (meta)-GGA functional including PBE, BEEF-vdW, SCAN, and SCAN+rVV10. For ethylene adsorption on noble metal Ag(111), it is found that BEEF-vdW, SCAN and SCAN+rVV10 predict the presence of the physisorption states only. For Rh(111), both SCAN and SCAN+rVV10 find that there is a precursor physisorption state before the chemisorption state. In contrast, there is no precursor state found based on potential energy surfaces from BEEF-vdW and PBE. Whereas for Ir(111), BEEF-vdW predicts the existence of a rather shallow precursor physisorption state, in addition to the chemisorption state. Irrespective to the transition metals considered, we find that SCAN+rVV10 gives the strongest binding strength, followed by SCAN, and PBE/BEEF-vdW, accordingly. The present work highlights great dependence of potential energy surface of ethylene adsorption on transition metal surfaces and exchange-correlation functionals.

Key words: Ethylene adsorption, Potential energy curve, Transition metal surface, Exchange-correlation functionals, First-principles theory

I. INTRODUCTION

The adsorption of molecule is a crucial elementary step that plays an important role in many fields, such as heterogeneous catalysis, electrochemistry, gas storage, and molecular sensors [1–5]. Depending on the adsorption strength and nature of molecular adsorption, the binding of molecules on the metal surfaces can be roughly classified as physisorption and chemisorption [6, 7]. In physisorption, van der Waals (vdW) forces are the dominant interactions accounting for the molecules bonding to the surfaces [8, 9], while chemisorption features the formation of chemical bonding in the type of either covalent or ionic [10, 11]. In heterogeneous catalysis, the adsorption of reactants on catalyst surface is the starting step in the reaction path, and this

has significant influence on the reaction process [12, 13]. For instance, it has shown that the selectivity of acetylene hydrogenation is strongly affected by the binding strength of the ethylene intermediate [14–16]. A weak binding of ethylene with catalysts will result in a fast desorption of ethylene once it is produced from acetylene hydrogenation on the catalyst surface, leading to a high ethylene selectivity in this reaction. Whereas the strong binding of ethylene would stay on the surface for sufficiently long time for furtherbeing hydrogenated with the formation of ethane as the main product. Therefore, the investigation of the adsorption and desorption process is essential for the understanding of reaction mechanism [17]. In practice, the molecular adsorption is normally accompanied with dramatic change in configuration and even bond breaking, which happens typically for strong chemisorption [18–21]. This process is often fast and difficult to be measured experimentally, a fact of that highlights the importance of theoretical study in particular via first-principles theory.

---

*Author to whom correspondence should be addressed. E-mail: wxli70@ustc.edu.cn

Density functional theory (DFT) calculations provide a promising way to elucidate molecular adsorption in-depth and have been proven to be effective in numerous previous studies [6, 22–28]. DFT can well describe in principle ground state properties of a multiple-electron system with exact electron density functional, which is however unknown yet or computational unaffordable otherwise. Therefore, in practice, computationally manageable approximations of the exact electron density functional are usually developed for the exchange-correlation energy E_{xc} [29–31]. The generalized gradient approximation (GGA) functionals integrating density gradients have been widely used to study the interaction between molecules and extended surfaces [32, 33, 33–35]. However, the GGA functionals such as the popular Perdew-Burke-Ernerhof (PBE) functional fail to capture well the vdW dispersion forces [36, 37]. It has been demonstrated that these vdW forces not only dominate the physisorption but also have a large impact on the chemisorption [8, 9]. Hence the absence of vdW in the functionals could result in inaccurate description of the adsorption properties, such as the adsorption energy. More accurate meta-GGAs have been developed, which incorporate kinetic energy density in exchange correlation energy. Among the meta-GGA functionals, the newly constructed strongly constrained and appropriately normed (SCAN) functional includes the intermediate-range vdW interaction [38]. The SCAN functional obeys all 17 known exact constraints and a set of "appropriate norms" including rare-gas atoms and nonbonded interactions [39]. This functional has shown its ability to much accurately predict the structures and energies of adsorbate-substrate systems where different types of bonding coexist [29]. A further improvement has been made by incorporating long-range vdW interaction and yields the so-called SCAN+rVV10 functional which has been verified to perform excellently in weak interactions [34]. However, the performance of SCAN+rVV10 in strong adsorption systems is still unclear. Moreover, a machine-learning based semiempirical method, namely the Bayesian error estimation functional with vdW correlation (BEEF-vdW), has been developed [40]. This method integrates an ensemble of functionals and analyzes uncertainties in a machine learning process. It has been shown that the BEEF-vdW could offer a reasonable reliability in description of vdW forces and quantitatively accurate prediction in chemical adsorption energies for molecules on surfaces [41].

Despite great efforts have been made to develop efficient and accurate exchange-correlation functionals, heretofore none of the functionals can universally describe all different type of interactions properly [37]. This has been well demonstrated for instance in benchmarking the calculated adsorption energy and molecular configuration *etc.* between calculation and measurement [6, 31]. During the adsorption process where the molecule approaches gradually the catalyst surface from the vacuum, the interaction between molecule and catalysts might change dramatically at different separation. Moreover, depending on the metal compositions, there might be a precursor state such as physisorption state occurring before reaching the final chemisorption state. There might be a barrier existing between the precursor state and final states. Since the different type of interactions are involved in adsorption process, which is true for the inverse desorption process, and could be metal-dependent, accurate description of this process would be a good touchtone on the exchange-correlation functional.

Ethylene adsorption process is important to the ethylene related heterogeneous catalytic reactions, such as syngas to olefins [42, 43], acetylene hydrogenation [14, 15, 44, 45], and ethylene epoxidation [46–48]. Thus, in this work, the adsorption process of ethylene from vacuum is systematically studied on the close-packed surfaces of transition metals (TMs). We considered three typical TMs of Ag, Rh, and Ir with different bonding strength (Ag versus Rh) and valence electron (4d Rh versus 5f Ir). Ethylene adsorption on these three metals widely involves different interaction types, from weak interaction on Ag to strong chemical bond with Rh and Ir. More importantly, ethylene adsorption on Rh and Ir can well represent two classical adsorption modes: π adsorption mode on Rh and di-σ adsorption mode on Ir. All these features about ethylene adsorption on different metals will be discussed in detail in the context. Four exchange-correlation functionals mentioned above, namely, PBE, BEEF-vdW, SCAN, and SCAN+rVV10, were employed for the DFT calculations. The results show that the potential energy surfaces of ethylene adsorption on transition metal surfaces are sensitive not only to metal composition but also to the exchange-correlation functionals used. This provides a value playground benchmarking the new exchange-correlation functional.

II. COMPUTATIONAL DETAILS

DFT calculations are performed by Vienna *ab initio* simulation package (VASP) [49, 50], and four different functionals are employed to describe the exchange-correlation interaction, namely PBE [32], BEEF-vdW [40], SCAN [39], and SCAN+rVV10 [34]. In the case of SCAN-based functionals, kinetic energy density including potential is implemented. The Kohn-Sham orbitals are extended in a plane wave basis with a cut-off energy of 400 eV. The convergence energy is set to be 1×10^{-4} eV. The close-packed (111) surfaces with p(2×3) unit cell for Ag, Rh, and Ir are modeled by slab models containing seven atomic layers. A (6×8×1) k-point mesh is used to sample the surface Brillouin zone, and a 20 Å vacuum is introduced in the repeated slabs along z-direction. During structural optimization, the bottom five layers of the slab are fixed, while the re-

maining atoms and the adsorbates in the x/y plane are fully relaxed until the residual forces are less than 2×10^{-2} eV/Å. It should be mentioned here that when potential surface energy of ethylene adsorption process is displayed, the height of carbon backbone of ethylene (coordinates in the z direction) is constrained to describe the height between the molecule and the metal surface metal.

The adsorption energy of ethylene at each fixed height is calculated as:

$$E_{\text{ads}} = E\left(\text{C}_2\text{H}_4, \text{TM}\right) - E\left(\text{C}_2\text{H}_4\right) - E\left(\text{TM}\right) \quad (1)$$

where $E(\text{C}_2\text{H}_4, \text{TM})$, $E(\text{C}_2\text{H}_4)$, and $E(\text{TM})$ are the total energies of the metal slab with adsorbed ethylene, ethylene molecule in gas phase, and the metal slab, respectively. For the transition states during adsorption transformation from physisorption to chemisorption, we have all verified them by the frequency calculations.

III. RESULTS AND DISCUSSION

A. Ethylene Adsorption on Ag(111)

The adsorption process is described here by the calculation of corresponding adsorption energy curve, which is plotted between the calculated adsorption energy and adsorption height. This height is defined as the distance between the carbon backbone of ethylene and the average height of the surface metal atoms. The adsorption energy curves predicted with different functionals for ethylene adsorption on Ag(111) surface are shown in FIG. 1. In the curve obtained using PBE functional, the almost constant adsorption potential energy of about -0.05 eV is observed when the adsorption height is larger than 3.20 Å (Table I). When the molecule height is smaller than 3.20 Å, the potential energy curve raises gradually as a decrease in the adsorption height due to the repulsive interaction between ethylene and Ag. This behavior makes no clear local minimum state present for ethylene adsorption on Ag, suggesting that PBE functional fails to describe the experimentally reported weak physisorption state for ethylene on Ag surfaces [46, 47, 51]. The reason might principally come from the lack of describing the vdW interaction in this functional.

The proper description of this weak physisorption can be significantly improved using BEEF-vdW, SCAN, and SCAN+rVV10 functionals. In the calculated potential energy curves from these functionals, it is downhill first but raises afterward as ethylene approaches the surface. This results in a clear local minimum, and the calculated adsorption energy using BEEF-vdW is -0.20 eV at the corresponding height of 3.49 Å, which remains too far away from the surfaces to form any pronounced bond. Different from BEEF-vdW, SCAN and SCAN+rVV10 predict a local minimum very similar but much closer to the surface at equilibrium height of
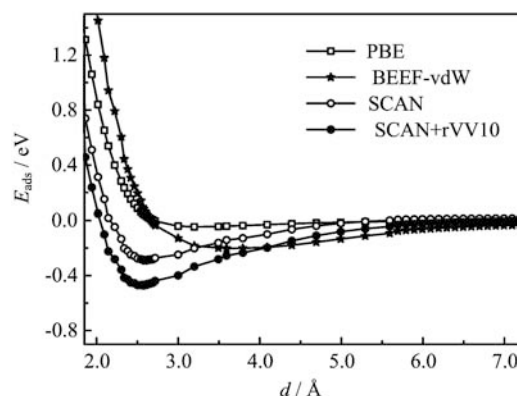
FIG. 1 Potential energy surface of ethylene adsorption on Ag(111) as a function of adsorption height d between ethylene and Ag surface from different exchange-correlation functionals.

TABLE I Adsorption energy (E_{ads} in eV), adsorption height (d in Å) at local equilibrium states (physisorption and chemisorption), and reaction barrier (E_{act} in eV) from physisorption to chemisorption for ethylene adsorption on Ag(111), Rh(111), and Ir(111) studied using different functionals.

Metal surface	Functionals	Physisorption		Chemisorption		
		E_{ads}	d	E_{ads}	d	E_{act}
Ag(111)	PBE	-0.05	3.20			
	BEEF-vdW	-0.20	3.49			
	SCAN	-0.29	2.56			
	SCAN+rVV10	-0.47	2.56			
Rh(111)	PBE			0.87	2.30	
	BEEF-vdW			-0.86	2.39	
	SCAN	-0.34	2.97	-1.27	2.12	0.17
	SCAN+rVV10	-0.51	2.97	-1.50	2.12	0.20
Ir(111)	PBE			-0.92	2.16	
	BEEF-vdW	-0.23	3.64	-0.87	2.18	0.07
	SCAN	-0.17	3.04	-1.43	1.99	0.49
	SCAN+rVV10	-0.35	3.04	-1.67	1.99	0.50

2.56 Å (FIG. 2(a)). The calculated adsorption energy is -0.29 eV and -0.47 eV for SCAN and SCAN+rVV10, respectively. The stronger binding strength for the latter one comes from the contribution of the long-range vdW interaction, which is not considered in the former one. We also considered DFT-D3 functional [52], and the calculated adsorption energy is -0.45 eV, very close to that of SCAN+rVV10.

To analyze the bonding nature of ethylene on Ag(111) surface, the electron localization function (ELF) of the adsorption structure at equilibrium state is studied. ELF is a simple measure of electron localization, reflecting the bonding feature between the adsorbate and substrate. The above results show that SCAN+rVV10 predicts the strongest binding strength for ethylene on
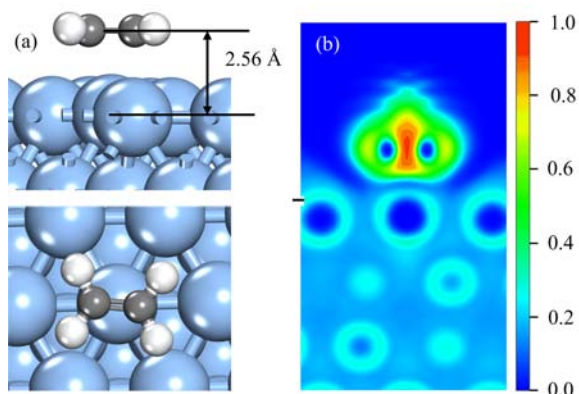
FIG. 2 (a) Most stable structure optimized using SCAN+rVV10 functional for ethylene adsorption on Ag(111). (b) The corresponding electron localization function (ELF). Color varying from blue to red indicates a gradual increase of extent of the electron localization. The blue, grey, and white balls represent Ag, C, and H atoms, respectively.

FIG. 3 Potential energy surface of ethylene adsorption on Rh(111) as a function of adsorption height d between ethylene and Ag surface from different xc-functionals.

Ag among four functionals considered, and thus the corresponding ELF is plotted in FIG. 2(b) to demonstrate the bonding nature. It is found that even in this closest distance and strongest binding from SCAN+rVV10, there is a little electron localization between ethylene and Ag. In-line with this weak interaction, the configuration of optimized ethylene on Ag is intact and same as the configuration of molecule in gas phase, and Bade charge calculation indicates that there is no charge transfer too.

B. Ethylene Adsorption on Rh(111)

FIG. 3 shows the potential energy curves for ethylene adsorption on Rh(111) surface. It can be found that both PBE and BEEF-vdW give only one local minimum state at equilibrium height of 2.30 Å and 2.39 Å, respectively. Corresponding adsorption energies are −0.87 eV for PBE and −0.86 eV for BEEF-vdW. We note that the calculated absolute binding strength is considerable and falls well in the range of formation of the chemical bond. For the formation of the strong chemical bond, the corresponding geometric and electronic structures of the adsorbate and substrate would be highly disturbed, compared to the reference state when the adsorbate is far away from the substrate as seen from FIG. 4 (a) and (c). In the chemisorption state (FIG. 4(c)), the molecular plane is dramatically destroyed and all the four hydrogen atoms are strongly repulsive by the metal surface with a dihedral angle of 147°. The large geometric and electronic rearrangement would raise the corresponding energy profile, which can lead to the formation of a saddle toward the chemisorption state and thus a so-called precursor state (possibly in a physisorption state) [6, 8, 9]. This precursor state and corresponding saddle point are however not found by PBE and BEEF-vdW,
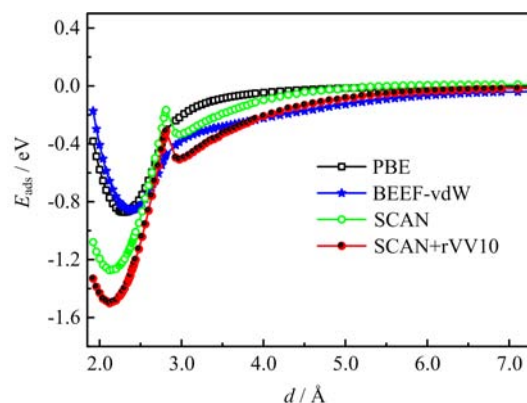
a fact of that indicates their deficiency in describing the strong chemisorption.

Different from PBE and BEEF-vdW, FIG. 3 shows that both SCAN and SCAN+rVV10 functionals predict two local minima in calculated potential energy surfaces. It is established that SCAN are sensitive to the structural transformation and could capture the small energy variation involved [29, 34]. The first minimum located at the adsorption height of 2.97 Å without observable structural changes for both functionals is assigned to the metastable precursor physisorption state (FIG. 4(a)). At this state, the calculated adsorption energies are −0.34 and −0.51 eV for SCAN and SCAN+rVV10, respectively. As ethylene approaches closer to the surface, a surface Rh atom is dragged out of the surface plane by forming C−Rh bond in a certain degree. This results in a rapid increase in energy profile and reaches a saddle point at height of 2.81 Å (FIG. 4(b)). The corresponding barrier for this process is 0.17 eV and 0.20 eV for SCAN and SCAN+rVV10, respectively. After crossing the saddle point, the second minimum state as the chemisorption state is approached. The calculated adsorption energy from SCAN+rVV10 is −1.50 eV, which is stronger than that of −1.27 eV from SCAN. The corresponding equilibrium height is 2.12 Å, which is much closer to the surfaces. As indicated in FIG. 4(c), this closer distance induces a pronounced structural rearrangement.

Different from the physisorption of ethylene on Ag, the nature of ethylene adsorption on Rh can be better presented by the corresponding ELF analysis. For the equilibrium structure optimized from SCAN, a strong electronic hybridization between ethylene and Rh at the chemisorption state is observed in the ELF (yellow area in FIG. 4(c)). This provides a clear evidence for the formation of covalent bonding with a characteristic of π-adsorption mode of ethylene with Rh underneath [11]. This strong π bond is supported by the obvious structural changes of the adsorbed ethylene. Specifically, the H−C bonds bend away from the plane of ethylene
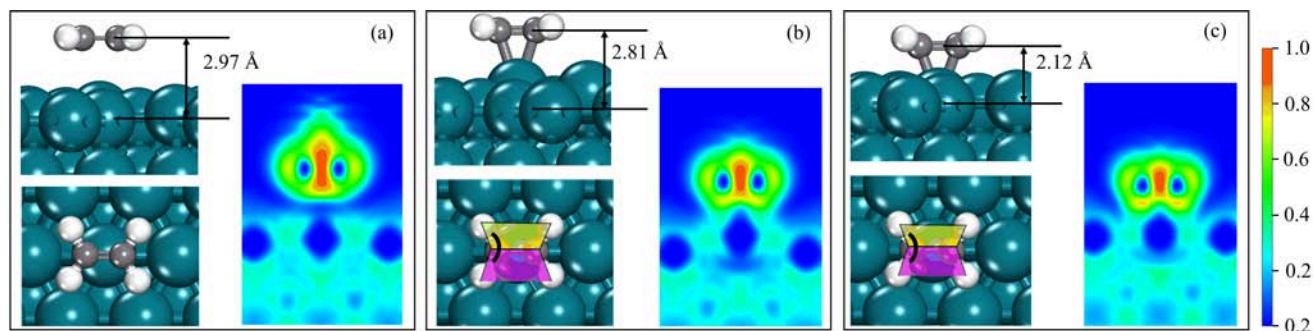
FIG. 4 Schematic structures (left) and corresponding electronic localization function (right) from SCAN: the precursor physisorption state (a), the transition state (b), and the chemisorption state (c) for ethylene adsorption on Rh(111). The dihedral angles of the H1−C−C−H2 and H3−C−C−H4 planes in ethylene are also indicated. The green, grey and white balls represent Rh, C, and H atoms, respectively.
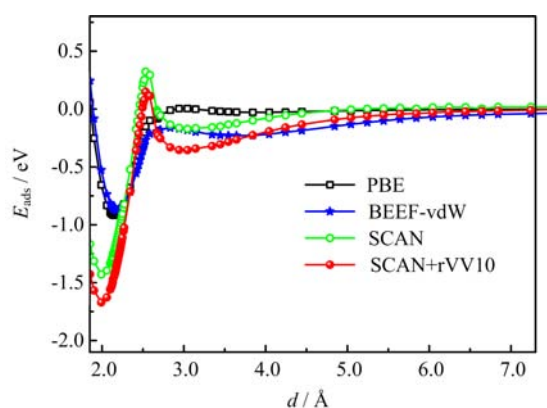
FIG. 5 Potential energy surface of ethylene adsorption on Ir(111) as a function of adsorption height d between ethylene and Ag surface from different xc-functionals.

molecule, resulting in a dihedral angle of 147° between the planes of H1−C−C−H2 and H3−C−C−H4. Moreover, the C−C bond in the adsorbed ethylene is elongated to 1.43 Å from 1.32 Å in the gas-phase ethylene. These structural variations indicate that the C atoms of ethylene have the tendency to rehybridize from sp^2 to sp^3, consistent with previous reports [18, 21, 53].

C. Ethylene Adsorption on Ir(111)

The adsorption energy profiles for ethylene on Ir(111) are depicted in FIG. 5, which are similar to those on Rh(111). There are two local minima in both SCAN and SCAN+rVV10 derived potential energy curves. The adsorption height on Ir(111) is 3.04 Å at the first local minimum (FIG. 6(a)), which is slightly larger than those of 2.97 Å on Rh(111). As a result, the corresponding physisorption on Ir with adsorption energy of −0.17 eV (SCAN) and −0.35 eV (SCAN+rVV10) is weaker than that on Rh (−0.34 and −0.51 eV). The predicted transition state from physisorption to chemisorption on Ir(111) surface exists only one imaginary frequency according to the vibrational analysis, which manifests the

stretch vibration of the new forming bonds between carbon atoms and the surface Ir atoms. This barrier is ∼0.50 eV, which is higher than that on Rh (less than 0.20 eV). Higher activation barrier comes from the larger structural rearrangement (FIG. 6(b)). First, the ethylene molecule at the transition state is closer to the surface with a height of 2.53 Å (SCAN), compared to that of 2.81 Å on Rh. Importantly, ethylene molecular plane exhibits a higher bending degree with a dihedral angle of 141° (FIG. 6(b)) between the planes of H1−C−C−H2 and H3−C−C−H4 from 180°, compared to that of 164° on Rh (FIG. 4(b)).

The chemisorption states for ethylene on Ir(111) are located at a height of 1.99 Å using SCAN and SCAN+rVV10, and the respective adsorption energies are −1.43 and −1.67 eV, which are 0.16 eV stronger than the corresponding values on Rh. Same as Rh, PBE cannot predict the existence of the precursor state yet. For BEEF-vdW, though it predicts the existence of the precursor state, the corresponding potential valley is extremely shallow with a barrier of 0.07 eV. Moreover, the calculated adsorption energy for the chemisorption state is −0.92 eV (PBE) and −0.87 eV (BEEF-vdW), which both are significantly higher than those from SCAN (−1.43 eV) and SCAN+rVV10 (−1.67 eV). Since ethylene adsorption on active metal surfaces is unstable, there are no available experimental data for comparison [54, 55]. Nevertheless, the calculated trend behavior is in good agreement with literature using similar functionals [56, 57].

For the chemisorption of ethylene on Ir(111), the ethylene molecule is covalently bonded to two adjacent surface Ir atoms (FIG. 6(c)). The di-σ adsorption mode on Ir [11] is different from that of π-adsorption mode on Rh. As seen from the corresponding ELF analysis, the adsorbed ethylene molecule suffers a larger structural change than that in π-adsorption mode. For SCAN optimized structure, the molecular plane of ethylene exhibits a higher degree of bending with a dihedral angle of 124° between the H1−C−C−H2 and H3−C−C−H4 planes. In addition, the C−C bond also exhibits an even
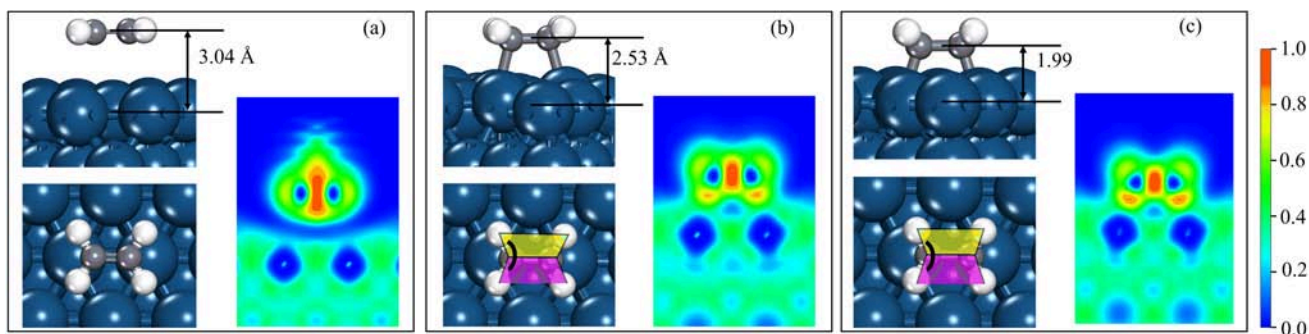
FIG. 6 Structures of SCAN optimized precursor physisorption state (a), transition state (b), and most stable state (c) for ethylene adsorption on Ir(111) with the corresponding ELF. The dihedral angles of the H1−C−C−H2 and H3−C−C−H4 planes in ethylene are also labeled. The blue, grey, and white balls represent Ir, C and H atoms, respectively.

longer bond distance of 1.50 Å, compared to that of 1.43 Å on Rh. These results suggest a deeper and more extensive rehybridization of C atoms from sp^2 to sp^3, in good agreement with the reported literature [19, 21, 58].

IV. CONCLUSION

The potential energy surfaces of ethylene adsorption on the close-packed surfaces of Ag, Rh, and Ir are studied by density functional theory using different exchange-correlation functionals including PBE, BEEF-vdW, SCAN, and SCAN+rVV10. On noble metal Ag(111), it is found that only PBE fails to predict the existence of the physisorption state of ethylene adsorption, due to the lack of the proper description of the vdW interaction. Whereas for the active 4d metal of Rh, both of PBE and BEEF-vdW functionals predict that there is only a chemisorption state available, whereas both SCAN and SCAN+rVV10 functionals find that there is in addition the presence of a physisorption state. For 5d metal of Ir, all functionals considered except PBE predict the presence of both physisorption and chemisorption states. Moreover, the transition barrier from the physisorption state to the chemisorption state on Ir(111) is larger than that of Rh(111). Irrespective to the transition metals considered, the present calculations show that SCAN+rVV10 gives the strongest binding strength, followed by SCAN, and PBE/BEEF-vdW, accordingly. The present work highlights great dependence of ethylene adsorption on transition metals for rationale of the catalyst design and exchange-correlation functionals used in density functional theory.

V. ACKNOWLEDGEMENTS

[1] D. A. King, Surf. Sci. **299-300**, 678 (1994).
[2] M. Frank and M. Bäumer, Phys. Chem. Chem. Phys. **2**, 3723 (2000).
[3] R. Waser and M. Aono, Nat. Mater. **6**, 833 (2007).
[4] N. Koch, A. Gerlach, S. Duhm, H. Glowatzki, G. Heimel, A. Vollmer, Y. Sakamoto, T. Suzuki, J. Zegenhagen, J. P. Rabe, and F. Schreiber, J. Am. Chem. Soc. **130**, 7300 (2008).
[5] C. Zhou, H. Shan, B. Li, and A. Zhao, Chin. J. Chem. Phys. **30**, 29 (2017).
[6] W. Liu, A. Tkatchenko, and M. Scheffler, Acc. Chem. Res. **47**, 3369 (2014).
[7] J. Ma, X. Yang, Y. Nie, and B. Wang, Phys. Chem. Chem. Phys. **20**, 9965 (2018).
[8] W. Liu, J. Carrasco, B. Santra, A. Michaelides, M. Scheffler, and A. Tkatchenko, Phys. Rev. B **86**, 245405 (2012).
[9] J. Carrasco, W. Liu, A. Michaelides, and A. Tkatchenko, J. Chem. Phys. **140**, 084704 (2014).
[10] R. Hoffmann, Rev. Mod. Phys. **60**, 601 (1988).
[11] C. Bernardo and J. Gomes, *Theoretical Aspects of Heterogeneous Catalysis*, Dordrecht: Springer, 217 (2001).
[12] S. Karakalos, Y. Xu, F. Cheenicode Kabeer, W. Chen, J. C. F. Rodrguez-Reyes, A. Tkatchenko, E. Kaxiras, R. J. Madix, and C. M. Friend, J. Am. Chem. Soc. **138**, 15243 (2016).
[13] P. Rodriguez, Y. Kwon, and M. T. M. Koper, Nat. Chem. **4**, 177 (2012).
[14] L. Xu, E. E. Stangland, and M. Mavrikakis, J. Catal. **362**, 18 (2018).
[15] F. Studt, F. Abild-Pedersen, T. Bligaard, R. Z. Sørensen, C. H. Christensen, and J. K. Nørskov, Science **320**, 1320 (2008).
[16] P. Wang and B. Yang, Chin. J. Catal. **39**, 1493 (2018).
[17] B. Xu, X. Liu, J. Haubrich, and C. M. Friend, Nat. Chem. **2**, 61 (2010).
[18] M. Li, W. Guo, R. Jiang, L. Zhao, X. Lu, H. Zhu, D. Fu, and H. Shan, J. Phys. Chem. C **114**, 8440 (2010).

[19] G. P. Petrova, G. N. Vayssilov, and N. Rösch, Catal. Sci. Technol. **1**, 958 (2011).

[20] A. S. Crampton, M. D. Rötzer, F. F. Schweinberger, B. Yoon, U. Landman, and U. Heiz, J. Catal. **333**, 51 (2016).

[21] C. J. Heard, S. Siahrostami, and H. Grönbeck, J. Phys. Chem. C **120**, 995 (2016).

[22] W. Zhao, S. M. Kozlov, O. Höfert, K. Gotterbarm, M. P. A. Lorenz, F. Viñes, C. Papp, A. Görling, and H. P. Steinrück, J. Phys. Chem. Lett. **2**, 759 (2011).

[23] A. Kundu, G. Piccini, K. Sillar, and J. Sauer, J. Am. Chem. Soc. **138**, 14047 (2016).

[24] Y. Sun, S. Zhang, W. Zhang, and Z. Li, Chin. J. Chem. Phys. **31**, 485 (2018).

[25] Z. Zhao, W. Lu, H. Zhu, W. Dong, Y. Lyu, T. Liu, X. Chen, Y. Wang, and Y. Ding, J. Catal. **361**, 156 (2018).

[26] C. Q. Huang and W. X. Li, Chin. J. Catal. **38**, 1736 (2017).

[27] S. Wang, M. Jian, H. Su, and W. Li, Chin. J. Chem. Phys. **31**, 284 (2018).

[28] J. Lin, H. Lv, and X. Wu, Chin. J. Chem. Phys. **31**, 649 (2018).

[29] J. Sun, R. C. Remsing, Y. Zhang, Z. Sun, A. Ruzsinszky, H. Peng, Z. Yang, A. Paul, U. Waghmare, X. Wu, M. L. Klein, and J. P. Perdew, Nat. Chem. **8**, 831 (2016).

[30] J. P. Perdew and K. Schmidt, AIP Conf. Proc. **577**, 1 (2001).

[31] S. Gautier, S. N. Steinmann, C. Michel, P. Fleurat-Lessard, P. Sautet, E. Normale, and S. De Lyon, Phys. Chem. Chem. Phys. **17**, 28921 (2015).

[32] J. P. Perdew, K. Burke, and M. Ernzerhof, Phys. Rev. Lett. **77**, 3865 (1996).

[33] C. F. Huo, Y. W. Li, W. Jianguo, and J. Haijun, J. Am. Chem. Soc. **131**, 14713 (2009).

[34] H. Peng, Z. H. Yang, J. P. Perdew, and J. Sun, Phys. Rev. X **6**, 041005 (2016).

[35] J. C. Liu, X. L. Ma, Y. Li, Y. G. Wang, H. Xiao, and J. Li, Nat. Commun. **9**, 1610 (2018).

[36] J. P. Perdew, MRS Bull. **38**, 743 (2013).

[37] A. Stroppa and G. Kresse, New J. Phys. **10**, 063020 (2008).

[38] J. P. Perdew, J. Sun, R. M. Martin, and B. Delley, Int. J. Quantum Chem. **116**, 847 (2016).

[39] J. Sun, A. Ruzsinszky, and J. Perdew, Phys. Rev. Lett. **115**, 036402 (2015).

[40] J. Wellendorff, K. T. Lundgaard, A. Møgelhøj, V. Petzold, D. D. Landis, J. K. Nørskov, T. Bligaard, and K. W. Jacobsen, Phys. Rev. B **85**, 235149 (2012).

[41] J. Wellendorff, T. L. Silbaugh, D. Garcia-Pintos, J. K. Nørskov, T. Bligaard, F. Studt, and C. T. Campbell, Surf. Sci. **640**, 36 (2015).

[42] H. M. Torres Galvis, J. H. Bitter, C. B. Khare, M. Ruitenbeek, A. I. Dugulan, and K. P. De Jong, Science **335**, 835 (2012).

[43] B. Wang, X. Yu, C. Huo, J. Wang, and Y. Li, Chin. J. Catal. **35**, 28 (2014).

[44] L. Wang, F. Li, Y. Chen, and J. Chen, J. Energy Chem. **29**, 40 (2018).

[45] F. Yao, Y. Huo, and Y. Ma, Chin. J. Chem. Phys. **30**, 559 (2017).

[46] X. L. Zhou and J. M. White, J. Phys. Chem. **96**, 7703 (1992).

[47] D. Stacchiola, G. Wu, M. Kaltchev, and W. T. Tysoe, Surf. Sci. **486**, 9 (2001).

[48] X. H. Lu, X. Che, Y. Q. Li, and Z. N. Wang, Chin. J. Chem. Phys. **24**, 311 (2011).

[49] G. Kresse and J. Furthmüller, Phys. Rev. B **54**, 11169 (1996).

[50] G. Kresse and J. Furthmüller, Comput. Mater. Sci. **6**, 15 (1996).

[51] L. Vattuone, L. Savio, and M. Rocca, Int. J. Mod. Phys. B **17**, 2497 (2003).

[52] S. Grimme, J. Antony, S. Ehrlich, and H. Krieg, J. Chem. Phys. **132**, 154104 (2010).

[53] H. J. Borg, R. M. Van Hardeveld, and J. W. (Hans) Niemantsverdriet, J. Chem. Soc. Faraday Trans. **91**, 3679 (1995).

[54] P. Sautet and J. F. Paul, Catal. Letters **9**, 245 (1991).

[55] S. Lizzit and A. Baraldi, Catal. Today **154**, 68 (2010).

[56] R. Shepard, S. Shepard, and M. Smeu, Surf. Sci. **682**, 38 (2019).

[57] A. Patra, J. Sun, and J. P. Perdew, ArXiv ID 1807.05450 (2018).

[58] C. J. Heard, C. Hu, M. Skoglundh, D. Creaser, and H. Grönbeck, ACS Catal. **6**, 3277 (2016).